Environment Canada
Environnement Canada

CANADA CENTRE FOR INLAND WATERS
CENTRE CANADIEN DES EAUX INTERIEURES

National Water Research Institute
Institut national de la recherche sur les eaux

THE DEPENDENCE OF THE AERODYNAMIC DRAG COEFFICIENT ON WAVE PARAMETERS

by

Mark A. Donelan

Canada

This manuscript was submitted as an
extended abstract to the First International
Conference on Meteorology and Air/Sea
Interaction of the Coastal Zone

THE DEPENDENCE OF THE AERODYNAMIC DRAG COEFFICIENT ON WAVE PARAMETERS

by

Mark A. Donelan

Shore Processes Section
Hydraulics Division
National Water Research Institute
Canada Centre for Inland Waters

February 1982

MANAGEMENT PERSPECTIVE

Calculations of wind-driven storm surges and lake circulations require a good estimate of the surface drag coefficient. This coefficient is not constant but is also a function of the waves.

Combined with an adequate wave prediction method, this paper provides a reliable means to estimate the drag coefficient, providing for the first time a real advance in the computation of wind set up, lake circulation and surface currents.

T. Milne Dick
Chief, Hydraulics Division
February 5, 1982

PERSPECTIVE DE GESTION

Le calcul des soulèvements de tempêtes par le vent et des courants de lac nécessite une bonne estimation du coefficient de traînée superficielle qui varie en fonction des vagues.

Jumelée à une méthode appropriée de prévision des vagues, cette communication s'avère un moyen fiable d'estimer le coefficient de traînée, et constitue un progrès réel dans le calcul des données sur le vent, des courants de lac et des courants de surface.

TABLE OF CONTENTS

THE DEPENDENCE OF THE AERODYNAMIC DRAG COEFFICIENT ON WAVE PARAMETERS

Mark A. Donelan

National Water Research Institute
Canada Centre for Inland Waters
Burlington, Ontario, Canada

1. INTRODUCTION

In a neutral turbulent boundary layer over a flat surface, there is ample evidence that the velocity profile follows the logarithmic "law of the wall" (Rotta, 1962).

$$U(Z) = \frac{u_*}{\kappa} \ln\left(\frac{Z}{Z_o}\right) \quad , Z_1 < Z < Z_2 \qquad (1)$$

Where u_* is the friction velocity, $\kappa=0.4$ is von Kármán's constant and Z_o is the roughness length or virtual origin of the logarithmic profile. Z_1 and Z_2 are heights such that the turbulent stress $\tau=-\rho\,\overline{u'w'} = \rho u_*^2$ is constant in magnitude and direction. In geophysical boundaries Z_1 and Z_2 define, respectively, the depth of the boundary layer affected by molecular viscosity and the depth relatively uninfluenced by the earth's rotation. Approximate values for Z_1 and Z_2 are given by Monin and Yaglom (1971) and Monin and Obukhov (1954) respectively:

$$Z_1 = 30\,\nu/u_* \qquad (2)$$

$$Z_2 = 0.01\,u_*/f \quad .$$

where f is the Coriolis parameter and ν is the kinematic viscosity.

In this region of the surface boundary layer, which over the ocean typically extends from heights of millimetres to tens of metres, the tangential stress τ may be estimated from the mean wind speed U(Z) and the roughness length Z_o, or equivalently the aerodynamic drag coefficient $C_D(Z)$.

$$\tau = -\rho\,\overline{u'w'} = \rho\,u_*^2 = \rho\,C_D(Z)\,U^2(Z) \qquad (3)$$

$$C_D(Z) = \left\{ \kappa / \ln\,(Z/Z_o) \right\}^2 \qquad (4)$$

The aerodynamic quality of the surface is classified according to the manner in which the tangential stress is communicated to the surface. The surface is said to be aerodynamically "smooth" if the stress is transmitted to the surface entirely through the agency of molecular viscosity and "rough" if the transfer is dominated by form drag on the roughness elements themselves. The transition between the two occurs as the viscous sublayer thins allowing the roughness elements to enter the turbulent boundary layer. A convenient classification, in terms of the roughness Reynolds number, $R_*=u_*Z_o/\nu$, has been established by experiment. Smooth flow corresponds to constant roughness Reynolds number ($R_* \approx 0.1$), while the flow is termed rough if $R_* > 2$. Roughness Reynolds numbers between these limits are indicative of transitional flow.

In boundary layers over solid (immobile) surfaces, the roughness length Z_o is related to the height, shape and spacing of roughness elements when the flow is aerodynamically rough. Generally, the more likely the roughness elements are to cause flow separation, the larger their influence on the roughness length. Typical values of the ratio of roughness length Z_o to height of roughness elements h_e vary from 1/30 for uniform sand grain roughnesses to 1/5 for typical agricultural crops (Monin and Yaglom, 1971). For example, Businger et al. (1971) find $Z_o \approx h_e/7.5$ for 18 cm high wheat stubble.

The description of the roughness length characteristic of a liquid surface is further complicated by the mobility of the roughness elements i.e. the waves. Typical values of the ratio of roughness length to the root mean square height of the waves are two orders of magnitude smaller than the values characteristic of a solid boundary. Various attempts to explain this have led to the conclusion that the roughness of the sea surface is due almost entirely to the short waves. Munk (1955) argued that the form drag of the surface is dominated by the short waves because of their relatively slow phase speeds and large contribution to the mean square slope of the surface. Charnock (1955) pointed out that, on dimensional grounds Z_o should be proportional to u_*^2/g. Phillips (1966) has related the root-mean-square height of the short waves to u_*^2/g and, since for rough flow Z_o is proportional to the height of the roughness elements, recovered Charnock's formula. Most of the experimental evidence available at the time suggested a nearly constant drag coefficient or one weakly dependent on wind speed in keeping with Charnock's model.

Kitaigorodskii and Volkov (1965) argued that the contribution of various wave components to the roughness length is affected by their phase speeds. In effect, the roughness length is proportional to the square root of the integral of the amplitude spectrum weighted by $\exp(-2\kappa c/u_*)$ where c is the component phase speed. For simplicity of application the self-similarity of the wind-generated spectrum is invoked (Kitaigorodskii, 1973) to relate the roughness length to the mean wave height, the phase speed of the spectral peak and the friction velocity.

New information on the role of wave breaking in inducing air flow separation (Banner and Melville, 1976; Gent and Taylor, 1976) caused Melville (1977) to relate the roughness length to the maximum amplitude of the waves with phase speed in the neighbourhood of the friction velocity.

Garrett's (1977) comprehensive review of the drag coefficient and the recent open ocean measurements of Smith (1980) and Large and Pond (1981) all

come down strongly in favour of a weak linear dependence of the drag coefficient on wind speed.

From a practical viewpoint it would be very convenient if the neutral drag coefficient could be determined solely from the surface wind speed. While such a relationship may do under the usual conditions of measurement of the surface stress (steady, long fetch), it is extremely unlikely to hold in general. In non-steady or inhomogeneous conditions, the roughness elements cannot be prescribed by the local wind only, but must be related to the characteristics of the wave field which may have been, to some extent, determined previously elsewhere.

Apart from the pioneering work of Kitaigorodskii and Volkov (1965) attempts to assess the effect of wave parameters on the stress have not been conclusive. Denman and Miyake (1973) and Large and Pond (1981) noticed increases in the drag coefficient in strengthening winds and following rapid changes in direction. Volkov (1970) and Davidson (1974) found appreciable wave effects on the stress. In particular, when the parameter c_p/u_* (the subscript "p" denotes the spectral peak) exceeded 25 the drag coefficient was reduced and, conversely, low values of c_p/u_* were associated with higher stresses. $c_p/u_*=25$ roughly corresponds to a fully developed sea, and here (Volkov, 1970) the effect on the drag coefficient of c_p/u_* was smallest.

Against the backdrop of controversy among air-sea interaction researchers must be placed the experience of storm surge modelers. The driving force for storm surge models is the wind stress; the desired output is the change in water level. The experience of modelers has been that high drag coefficients are required to bring the model output into reasonable agreement with observations. Figure 1 compares the choice of drag coefficient of some modelers with the results of air-sea interaction experiments. Platzman (1963) used a value of 0.003 to apply to wind measurements around Lake Erie. The line (P) shown in Figure 1 spans the range of peak wind speeds covered by the nine storms studied. Heaps (1969) (H) and Timmerman (1977) (T) use two very different formulas for the drag coefficient although both were developed for North Sea storm surges. However the difference is not large above 14 m/s where the water level responses are appreciable. Garratt (1977) summarized the drag coefficient measurements over water and found that linear regression on wind speed yielded a neutral drag coefficient referred to 10 m height $C_{DN}(10)$ of:

$$C_{DN}(10) \times 10^3 = 0.75 + 0.067\, U(10); \quad \text{for } 4 < U(10) < 21 \text{ m/s} \qquad (5)$$

However, Garratt lumped profile and eddy correlation data together and the few measurements above 16 m/s are taken from the Sable Island experiment of Smith and Banke (1975). At these higher wind speeds the waves approaching the island were shoaling and were certainly not representative of deep water waves. Since there are some questions about the use of the profile technique over water, we have recomputed the regression line for the eddy correlation data only between 4 m/s and 16 m/s. The result is:

$$C_{DN}(10) \times 10^3 = 0.96 + 0.041\, U(10); \quad \text{for } 4 < U(10) < 16 \text{ m/s} \qquad (6)$$

and is shown as G' on Figure 1. There are 370 observations included and the correlation coefficient is 0.65. Since Garratt's review, the open ocean observations of Smith (1980) and Large and Pond (1981) have appeared. These are indicated in Figure 1 by (S) and (L&P). Smith's result is based on 63 observations under neutral long fetch conditions. Large and Pond based their result on 1591 hourly estimates of the stress using the dissipation method, which they had checked against eddy correlation data.

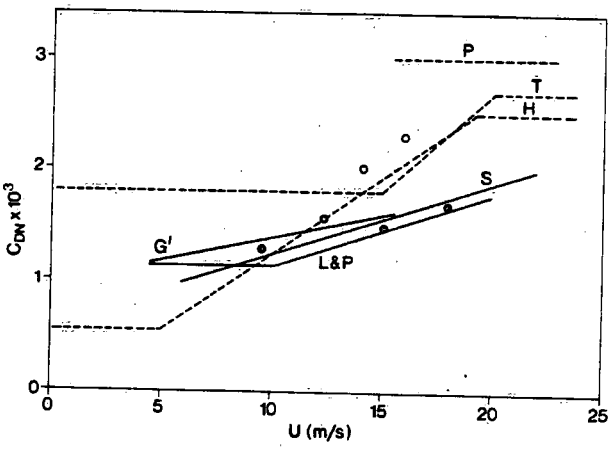

Figure 1. The neutral drag coefficient C_{DN} versus wind speed U from other sources. The solid lines are regression lines from eddy correlation estimates of $\overline{u'w'}$; the dashed lines are the formulae adopted by three storm surge modelers; the solid circles are derived from the water level fluctuations over several months (Schwab, 1981); the open circles are derived from the peak storm surge for two storms (Simons, 1974 and 1975).

It would appear that the experimental results are in general agreement with each other but not with the storm surge model requirements. It may be argued that the inaccuracies involved in using overland winds (Platzman) or surface pressure maps (Heaps and Timmerman) may be at the root of the difference. However, in recent years hydrodynamic models have been applied to Lake Ontario (Simons, 1974 and 1975) and to Lake Erie (Schwab, 1981) using wind observations from several meteorological buoys distributed over the lake. Schwab used an inverse method to deduce the wind stress from the water level fluctuations. He applied his method to continuous observations from May to October 1979 and determined the neutral drag coefficient (at the wind measuring height of 4 m) in four wind speed classes. His results, adjusted to 10 m, are also indicated in Figure 1. Simons modeled two storms with peak 4 m wind speeds of 12.9 and 14.4 m/s. In both cases he used $C_{DN}(4)=0.0025$. The water levels were well modeled for the 12.9 m/s storm but underestimated for the other. The values of his drag coefficient adjusted to 10 m and, in the 14.4 m/s storm, adjusted to improve the match to the observed water levels are indicated in Figure 1.

Schwab's seven-month average drag coefficients are weighted towards steady conditions, whereas Simons' pertain to the peaks of storms. The fact that Schwab's coefficients fall in line with the eddy correlation results is reassuring evidence that the eddy correlation method correctly estimates the total wind stress. The fact that Simons' coefficients are much

larger and more closely allied with the choices of other storm surge modelers suggests that rapidly changing winds induce higher tangential stresses than steady winds. The most likely agency to bring about such a change in the apparent roughness is the wave field.

Evidently the believable measurements of surface stress are heavily biased towards long fetch and steady conditions leading to full or nearly full wave development. In order to extract useful information on wave effects among the experimental noise and sampling variability characteristic of the measurement of $\overline{u'w'}$, an observational program was designed to acquire stress estimates while the waves were in various stages of development. This paper describes the results of those measurements and suggests a model for the drag coefficient which includes the effects of mobility of the roughness elements. The model bears a family resemblance to that of Kitaigorodskii and Volkov (1965), but differs from it in that the wave spectrum is separated into two parts: the equilibrium range which is assumed to have an average direction parallel with the wind; and the peak which need not be in the wind direction.

2. OBSERVATIONS

The measurements were made from a tower fixed to the bottom in 12 m of water at the western end of Lake Ontario. From this point the tower commands fetches of 1.1 km to 300 km. At approximately 11 m above the surface the turbulent momentum flux was measured by a Gill anemometer-bivane. The parameters measured by this instrument are the wind vector magnitude, azimuth and elevation from which the velocity components may be computed. Wave measurements were made with a capacitance wave gauge (4.8 mm diameter) with a resolution of 1.5 mm. The direction of wave approach was estimated using the method given by Donelan (1980) based on directional spectra obtained at this site. Air and water surface temperatures were obtained with thermistors and a thin film capacitor ("Humicap") provided relative humidity information.

All these data were sampled at 5 Hz and transmitted digitally by cable to a mini-computer on the shore. The averaging time for wave and stress estimates was set at 20 minutes, since this is near the centre of the spectral valley between meso- and microscale wind turbulence regions. A linear trend was computed and removed from all the data before computation of fluxes or variances. Consecutive 20 minute averages of $\overline{u'w'}$ contain sampling variability in excess of 30 percent. To reduce this variability the drag coefficients reported here are computed from the average of three consecutive 20 minute estimates of $\overline{u'w'}$ divided by the square of the wind speed averaged in the same way.

3. STABILITY EFFECTS

These data cover a range of stability of $-0.05 \leq R_b \leq 0.02$; where R_b is the bulk Richardson number. Donelan et al. (1974) found an empirical connection between R_b and Z/L (the Monin-Obukhov stability index) using the results of Businger et al. (1971). When the corrections to the stability functions of Businger et al. suggested by Wieringa (1980) have been applied, the result of Donelan et al. (1974) becomes:

$$Z/L = 7.6\, R_b \quad , \quad R_b < 0$$
$$Z/L = 6.0\, R_b \quad , \quad R_b > 0 \qquad (7)$$

and the stability range of these data is $-0.38 \leq Z/L \leq 0.12$. The bulk Richardson number was computed from the data and (7) used to estimate Z/L. The method described by Large and Pond (1981) was then applied to yield $C_{DN}(10)$, and U(10). u_* and Z_o follow from (3) and (4). The equivalent 10 m wind speed for neutral stability $U_N(10)$ follows from (1). Anticipating a later result, we find that the ratio of $C_{DN}(10)$ to the modeled value $\tilde{C}_{DN}(10)$ is uncorrelated with R_b (correlation coefficient r=0.03). This implies that the stability correction was valid. There were 153 independent hourly estimates of $C_{DN}(10)$ in the wind speed range $4 < U(10) < 17$ m/s.

4. ROUGHNESS

In the light of the discussion in section 1, we examine the data in terms of roughness Reynolds number (Figure 2). Using the criteria established for solid boundaries 78% of the data are in fully rough flow and 94% are either rough or transitional. Two differences from solid boundaries are immediately apparent: five points are at appreciably lower values of R_* than the condition for smooth flow ($R_* \approx 0.1$); the roughness length Z_o is not linearly proportional to the height of the surface irregularities for fully rough flow ($R_* > 2$). A plausible explanation for the ultra-smoothness ($R_* < 0.1$) of the surface is that some components of the wave field are travelling faster than the wind and transferring momentum to the boundary layer. At the other end of the roughness scale, the ratio of roughness length to the mean* height $\bar{H}$ of the waves approaches the value characteristic of sand grain roughnesses: 1/30. Evidently at large values of the roughness Reynolds number ($R_* > 50$), the surface approaches the roughness of a solid surface with similar size roughness elements. Since the measure of roughness ($\bar{H}$) is strongly dominated by the long waves near the spectral peak this implies that a large fraction of the total stress is caused by flow separation from the crests of these waves. Kitaigorodskii (1973) has argued that this should be the case in the initial stage of wave development when all the wave components are travelling slowly compared to the local wind.

Melville (1977) has argued that the transition from smooth to rough flow should occur when the friction velocity exceeds the phase speed of the slowest waves (23 cm/s). The points on Figure 2 associated with values of u_* less than 23 cm/s are indicated (Δ). While all the ultra-smooth values fall into this category, there seems to be no particular stratification of the data above and below $u_* = 23$ cm/s. In particular, the independence of Z_o on the surface features - characteristic of smooth flow - is not evident. Rather, all the data seem to fall in with a general trend of increasing $Z_o/\bar{H}$ with roughness Reynolds number.

*Here we use Longuet-Higgins' (1952) result for a narrow spectrum $\bar{H} = \sqrt{2\pi}\,\sigma$ where σ is the root-mean-square surface deviation.

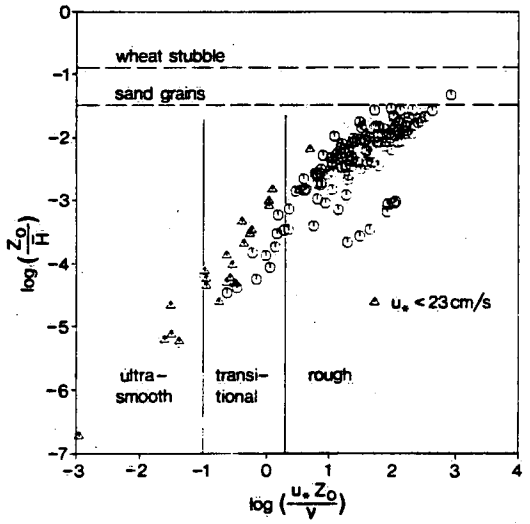

Figure 2. The variation of the ratio of roughness length to mean wave height with roughness Reynolds number, R_*. The regions of R_* corresponding to various types of flow over a solid surface are indicated. The ordinate values corresponding to sand grains and wheat stubble are indicated.

Kitaigorodskii (1973) has examined the effect of mean wave steepness on this ratio and found no significant correlation both before and after he had accounted for the mobility of the waves. This may be because the steepness of the slowly moving waves approaches an equilibrium value limited by breaking. At short fetch the waves at the peak of the spectrum fall into this category and as the spectrum approaches full development the waves near the spectral peak become less steep, but at the same time their contribution to the stress is greatly diminished by their increased speed. Thus, whereas in all cases the stress is caused by waves approaching limiting steepness, the mean steepness is largely a function of the steepness of the waves near the spectral peak.

The circumstance that the roughness length characteristic of steady long fetch measurements is anomalously small is the primary piece of evidence in support of the widely held view that the form drag is due to the short waves. The Charnock formula is, in effect, a corollary of this and, among the generous scatter of drag coefficient estimates, has nestled rather more comfortably than deserved. Figure 3 is a scatter diagram of Z_0 versus u_*^2/g on logarithmic scales. For dimensional correctness the data should indicate a slope of 1:1. The straight line is one such expression of Charnock's formula - using Garratt's α=0.0144. Kitaigorodskii (1973) has pointed out that the Charnock "constant" should be dependent on roughness Reynolds number and state of wave development. The data have been classified by state of wave development represented by the ratio of wind speed U(10) to phase speed of the spectral peak c_p. At high values of U/c_p the data approach a 1:1 slope, but with a much higher Charnock parameter ($\alpha \approx 0.04$). At lower values of U/c_p characteristic of the open ocean measurements, the dimensionality arguments, which led to the Charnock formula, are clearly insufficient to describe the process. While it may be possible to model the surface roughness adequately by determining an explicit dependence of the Charnock parameter on other mean properties of the interface, there would seem to be little to be gained thereby in our understanding of the drag on a water surface. Rather, we choose to make use of the observable characteristics of the surface to construct a model which approaches the limits of (a) flow over a comparable rough solid surface for very young waves, and (b) no net form drag on the large waves as they approach full development.

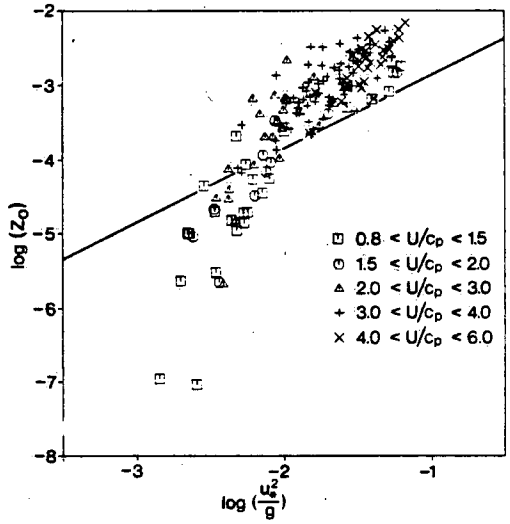

Figure 3. The variation of roughness length Z_0 (m) with u_*^2/g. The line shown, of unit slope, corresponds to the Charnock relation with Garratt's (1977) estimate of α=0.0144. The symbols denote different stages of development of the wave spectrum as shown.

5. THE MODEL

For comparison with the model results (to follow) the data are graphed in Figure 4 according to the prevailing fashion - drag coefficient $C_{DN}(10)$ versus wind speed U(10). While the correlation coefficient of the linear regression line is quite respectable (r=0.72), it is clear that a linear dependence on wind speed describes the data inadequately. Further, the regression line of Figure 4

$$C_{DN}(10) \times 10^3 = 0.37 + 0.137\, U(10); \quad \text{for } 4 < U(10) < 17 \text{ m/s} \tag{8}$$

is markedly different from the other empirical results (Figure 1). It can be seen from the stratification of the points of Figure 4 that the difference is due to the short fetch or high U/c_p cases. It is tempting to associate these high values of U/c_p with the transient conditions to which storm surge models are tuned, and the low values of U/c_p with the characteristic conditions of long fetch air-sea flux measurements.

Banner and Melville (1976) and Gent and Taylor (1976) demonstrated that flow separation of a mean air streamline from the surface requires a stagnation point on the surface in a frame of reference travelling at the phase speed. The fact that this occurs during wave breaking establishes a link between form drag and wave breaking. In a laboratory experiment Banner and Melville found that the drag on a wavy water surface increased dramatically when the

wave was caused to break. Consequently, a realistic model for the drag on an aerodynamically rough water surface must take cognizance of the breaking process.

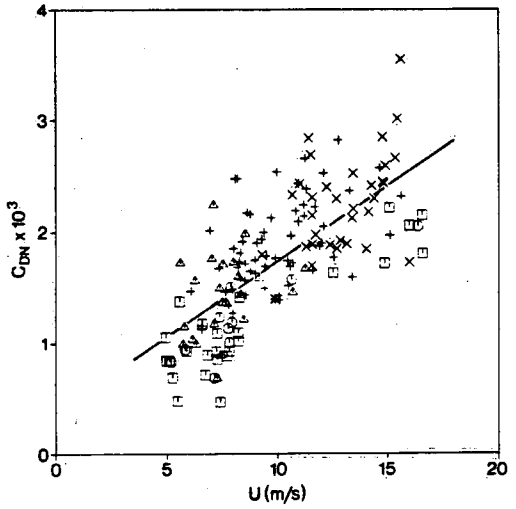

Figure 4. Neutral drag coefficient estimates C_{DN} plotted against wind speed U. Each estimate is derived from an average of three consecutive 20 minute measurements of $\overline{u'w'}$. These symbols have the same meaning as in Figure 3. The linear regression line for these data is indicated.

Melville (1977) proposed a model for the roughness length based on the premise that the roughness elements are the small scale breaking waves for which $c \approx u_*$. It is a matter of common observation that breaking occurs at the crests of the large waves in a wind-generated sea. These, generally spilling - sometimes plunging, breakers entrain air and produce foam - "whitecaps". However, breaking on a less dramatic scale must go on over much of the equilibrium range of the wave spectrum. Apparently the variation of the equilibrium range (Phillips) parameter with non-dimensional fetch (Hasselmann et al., 1973) must reflect a balance between dissipation through breaking and wind input enhanced by breaking. It is to these small waves that Melville's arguments apply. The excellent set of sea state photographs from ocean weather station "P" (Allen, 1968) illustrate both scales of breaking. At Beaufort Force 6 ($U(10) \approx 12$ m/s) and above, the importance of flow separation from the large waves cannot be in doubt. Additional evidence for the increased form drag during breaking comes from the observations of spectral peak enhancement at short fetches (Hasselmann et al., 1973, Donelan et al., 1982). For such spectra, calculations indicate that nonlinear wave-wave interaction (Hasselmann et al., 1973) adds energy to the low frequencies and high frequencies at the expense of the peak and the frequencies just above. Whitecaps at the crests of the large waves imply energy dissipation near the peak of the spectrum. In spite of these the spectral peak is enhanced, which suggests that the energy (and momentum) transfer from the wind to the waves at the peak of the spectrum must be particularly large at these fetches.

Let us now examine that which we know or can reasonably deduce from the available evidence with the aim of using it to construct the simplest model which will allow us to estimate the drag on a water surface from the averages of first order quantities. We know that flow separation and wave breaking are closely linked and that wave breaking occurs at the crests of the waves near the spectral peak and also less dramatically over most of the equilibrium range. We know that the roughness length is generally a very small fraction of the wave height, but approaches the value corresponding to certain solid boundaries when the roughness Reynolds number is large. Furthermore, the surface sometimes appears to be ultra-smooth. These last two effects are, we believe, due to the mobility of the roughness elements (waves). We know that the waves near the spectral peak can, in fetch-limited (Donelan, 1980) or non-stationary (Hasselmann, 1980) conditions, be travelling at off-wind angles. On the other hand, the shorter waves in the equilibrium range are generally quite closely aligned with the wind.

Thus as a collection of travelling roughness elements the spectrum of surface waves is conveniently separated into two parts: (1) the peak - characterized by enhancement, whitecaps, and off-wind travel; (2) the equilibrium range - characterized by quasi-saturation, micro-breaking* and down-wind travel. The criterion for separation of these two types of roughness elements is somewhat arbitrary, but we note that the spectrum (Hasselmann et al., 1973; Donelan et al., 1982), above the enhanced peak, undershoots before approaching the equilibrium range level near $\omega = 2\omega_p$, where ω_p is the frequency of the spectral peak. Therefore, we select the frequency $2\omega_p$ as the dividing line between long and short waves. Each component (long or short) is assumed to have an equivalent immobile surface roughness length Z_i proportional to the root-mean-square height of the waves in the appropriate part of the spectrum. That is:

$$Z_\ell = \beta \left[\int_0^{2\omega_p} E(\omega)\, d\omega \right]^{1/2}$$

$$Z_s = \beta \left[\int_{2\omega_p}^{\infty} E(\omega)\, d\omega \right]^{1/2} \qquad (9)$$

where $E(\omega)$ is the frequency spectrum, the subscripts ℓ and s refer to long and short waves and β is a constant of proportionality of order 10^{-2} to 10^{-1} to be determined empirically. If the surface were frozen at some instant in time the contribution to the total surface stress for each component would be given by substituting (9) in (4). However, both components travel at some appreciable fraction of the wind speed and thus the apparent drag coefficient estimated by a fixed observer is altered as follows:

$$\left[C_D\right]_\ell = \left[\hat{C}_D\right]_\ell \cdot |\cos\theta| \cdot \left|U_N - \frac{c_\ell}{\cos\theta}\right| \cdot \left(U_N - \frac{c_\ell}{\cos\theta}\right)/U_N^2$$

$$\left[C_D\right]_s = \left[\hat{C}_D\right]_s \cdot (U_N - c_s)^2 / U_N^2 \qquad (10)$$

where $\hat{}$ signifies the equivalent immobile surface drag coefficient; θ is the angle between the wind and the waves at the spectral peak; the factor $|\cos\theta|$ accounts roughly for the reduction in drag as the

*Micro-breaking is used here to mean breaking which is too gentle to produce a discernible colour change (insignificant air entrainment), but in which, nonetheless, the fluid just ahead of the crest advances relative to the crest.

waves move away from the wind direction. c_ℓ and c_s are characteristic speeds of the wave components. Observational evidence (Bretschneider, 1973) indicates that the spectrum becomes fully developed when $U/c_p = 0.83$. At full development the waves near the peak of the spectrum are less steep and break infrequently. Thus we assume that under these conditions the long waves contribute nothing to the total drag and therefore choose* $c_\ell = 0.83\, c_p$. Or using the linear theory dispersion relation $c_\ell = 0.83 g/\omega_p$. For consistency $c_s = 0.83 g/2\omega_p$. The wind speed U_N is the equivalent neutral wind speed at 10 m from (1).

The model contains one parameter, β, which must be determined by comparison with the data but which, by analogy with flow over solid surfaces, is of order 10^{-2} to 10^{-1}. The estimates of hourly average neutral drag coefficients $C_{DN}(10)$ were compared with the model coefficients $C_{DM}(10)$ for various values of β.

$$\text{where } C_{DM}(10) = \left[C_D\right]_\ell + \left[C_D\right]_s \qquad (11)$$

The best agreement between model and observations was obtained with $\beta = 1/80$. For this value of β the correlation coefficient $r = 0.79$.

In building this model based on the idea of flow separation from breaking waves, we have related the equivalent immobile surface roughness lengths Z_ℓ and Z_s to the heights of the waves in various parts of the spectrum. However, the degree of whitecap coverage increases with the wind speed (Monahan, 1969) and also with the wave height. Thus, we would expect the form drag on the waves to increase with whitecap coverage in addition to the behaviour modeled in (9) and (10). To test this the ratio $C_{DN}(10)/C_{DM}(10)$ was regressed against the logarithm of a sea-state Reynolds number $R_s = U_N \sigma/\nu$; where σ is the total root-mean-square surface deviation and ν is the kinematic viscosity of the air. These parameters are weakly correlated ($r = 0.32$) possibly because of the noise inherent in the hourly C_{DN} estimates. Nonetheless, the regression equation can be used to make a further small adjustment to the model drag coefficient values:

$$\tilde{C}_{DM} = C_{DM} \times (0.07 + 0.2 \log R_s) \qquad (12)$$

The hourly average neutral drag coefficient estimates, C_{DN} are graphed against the final modeled values $\tilde{C}_{DM}$ in Figure 5. The application of (12) improved the correlation coefficient to $r = 0.82$.

The scatter of the points about the 45° line is still rather large. Some of it is undoubtedly due to the sampling variability of the hourly average estimates of C_{DN}. In an effort to determine this component of noise, we examined the variability of the hourly estimates about longer (10 to 17 hours) averages of C_{DN} under steady conditions, and found that the standard deviation of the hourly averages about these longer term averages was 15% on average. Since the distribution of the hourly estimates about their mean was nearly normal, we can place confidence limits on the model prediction (45° line). The 90% and 95% confidence limits are shown on Figure 5. The 90% limits enclose 80% of the data and the 95% limits enclose 88% of the data. Apparently the discrepancy between model and observations could be due almost entirely to the observational variability of C_{DN}. There is no doubt that the model is an imperfect facsimile of the natural process, and the mean measurements required to construct the model have themselves some error. However, it would appear that the variability of the measurements of C_{DN} account for most of the difference between model and measurement.

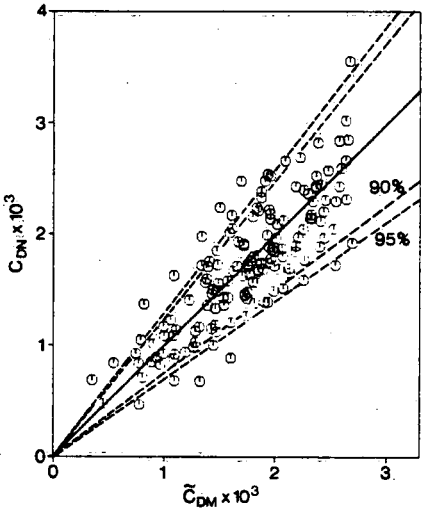

Figure 5. Neutral drag coefficient estimates C_{DN} compared with the modeled values $\tilde{C}_{DM}$. The line of perfect agreement is shown (solid) as are the 90% and 95% confidence limits (dashed) based on the sampling variability of C_{DN}.

6. FINAL REMARKS

We have demonstrated that a model, which includes the mobility of the waves, accounts for most of the variability of the drag coefficient save that which is apparently due to sampling variability. We have argued that the difference in values provided or used by various researchers can be ascribed to the state of wave development. We may exercise the model (9), (10), (11) and (12) for various states of wave development (U/c_p values) and plot the results against U(10) to compare with the empirical results of others (Figure 6). The open ocean data of Smith (S) and Large and Pond (L &P) fall between $U/c_p = 1.0$ and $U/c_p = 1.5$. That is, their data approach full development. These values of U/c_p correspond to dimensionless fetches in the range 7×10^3 to 4×10^4 (Donelan et al., 1982) and are characteristic of long fetch data. Interestingly Smith and Banke's Sable Island data (S&B) do not follow the slope of the other curves, but increase in a manner consistent with a relative increase of U/c_p with wind speed. If the waves in deep water approaching Sable Island were nearly fully developed, this is just the effect that shoaling would produce - affecting the long waves (high wind speed) more than the short, both in retardation and breaking.

ACKNOWLEDGEMENTS

I am grateful to D. Beesley, J. Carew, E. Harrison and H. Saville for assistance with the field program. A. El-Shaarawi, P. Hamblin, G. Ivey and J. Simons offered useful comments and criticisms.

*We have assumed that $\theta = 0$ for the full development data from which Bretschneider's condition ($U/c_p = 0.83$) was obtained. This assumption is consistent with the requirment of unlimited fetch and steady conditions implicit in the idea of full development.

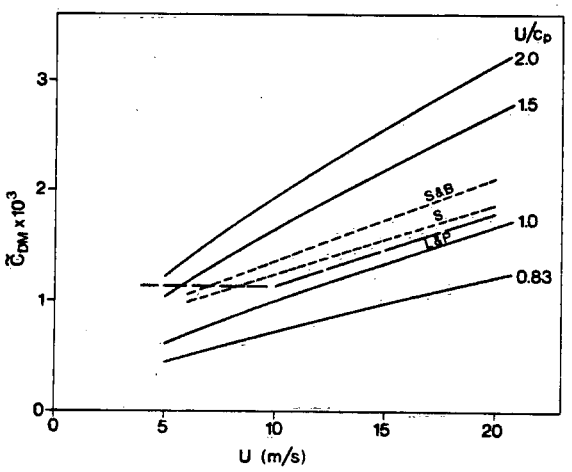

Figure 6. Model drag coefficients $\tilde{C}_{DM}$ plotted versus wind speed for various stages of wave development. The wave characteristics required for input to the model are obtained through hindcasting formulae Donelan (1980). Some empirical drag coefficient regression lines are added for comparison.

REFERENCES

Allen, W.T.R., 1968: State of sea photographs for the Beaufort wind scale. Queen's Printer, Canada, 49 pp.

Banner, M.L., and W.K. Melville, 1976: On the separation of air-flow over water waves. J. Fluid Mech., 77, 825-842.

Bretschneider, C.L., 1973: Prediction of waves and currents. Look Lab/Hawaii, 3.1, 17 pp.

Businger, J.A., J.C. Wyngaard, Y.K. Izumi, and E.F. Bradley, 1971: Flux-profile relationships in the atmospheric surface layer. J. Atmos. Sci., 28, 181-189.

Charnock, H., 1955: Wind stress on a water surface. Quart. J. Roy. Meteor. Soc., 81, 639-640.

Davidson, K.L., 1974: Observational results on the influence of stability and wind-wave coupling on momentum transfer and turbulent fluctuations over ocean waves. Bound.-Layer Meteor., 6, 305-331.

Denman, K.L., and M. Miyake, 1973: The behaviour of the mean wind, the drag coefficient, and the wave field in the open ocean. J. Geophys. Res., 78, 1917-1931.

Donelan, M.A., K.N. Birch, and D.C. Beesley, 1974: Generalized profiles of wind speed, temperature and humidity. Internat. Assoc. Great Lakes Res., Conf. Proc. 17, 369-388.

Donelan, M.A., 1980: Similarity theory applied to the forecasting of wave heights, periods and directions. Proc. of Cdn. Coastal Conf. 1980, 47-61.

Donelan, M.A., J. Hamilton, and W.H. Hui, 1982: Directional spectra of wind-generated waves, (In prep.).

Garratt, J.R., 1977: Review of drag coefficients over oceans and continents. Mon. Wea. Rev., 105, 915-929.

Gent, P.R., and P.A. Taylor, 1976: A note on "separation" over short wind waves. Bound.-Layer Meteor., 11, 65-87.

Hasselmann, D.E., M. Dunkel, and J.A. Ewing, 1980: Directional wave spectra observed during JONSWAP 1973. J. Phys. Ocean. 10, 1264-1280.

Hasselmann, K., T.P. Barnett, E. Bouws, H. Carlson, D.E. Cartwright, K. Enke, J.A. Ewing, H. Gienapp, D.E. Hasselmann, P. Kruseman, A. Meerburg, P. Muller, D.J. Olbers, K. Richter, W. Sell, and H. Walden, 1973: Measurements of wind-wave growth and swell decay during the Joint North Sea Wave Project (JONSWAP). Deut. Hydrogr. Z., Suppl. A, 8, No. 12, 22 pp.

Heaps, N.S., 1969: A two-dimensional numerical sea model. Phil. Trans. A, 265, 93-137.

Kitaigorodskii, S.A., and Yu A. Volkov, 1965: On the roughness parameter of the sea surface and the calculation of momentum flux in the near-water layer of the atmosphere. Izv. Atmos. Oceanic. Phys., 1, 973-988.

Kitaigorodskii, S.A., 1973. The physics of air sea interaction. (Israel Program for Scientific Translations, Jerusalem, 237 pp.)

Large, W.G., and S. Pond, 1981: Open ocean momentum flux measurements in moderate to strong winds. J. Phys. Ocean. 11, 324-336.

Longuet-Higgins, M.S., 1952: On the statistical distribution of the heights of sea waves. J. Mar. Res., 11, 245-266

Melville, W.K., 1977: Wind stress and roughness length over breaking waves. J. Phys. Ocean., 7, 702–710.

Monahan, E.C., 1969: Fresh water whitecaps. J. Atmos. Sci., 26, 1026-1029.

Monin, A.S., and A.M. Obukhov, 1954: Basic laws of turbulent mixing in the ground layer of the atmosphere. Akad. Nauk. SSSR Geofiz. Inst. Tr., 151, 163-187.

Monin, A.S., and A.M. Yaglom, 1971. Statistical Fluid Mechanics, Vol. 1, The MIT Press, Cambridge, 769 pp.

Munk, W., 1955: Wind stress on water: an hypothesis. Quart. J. Roy. Meteor. Soc., 81, 320-332.

Phillips, O.M., 1966: The dynamics of the upper ocean. Cambridge University Press, 261 pp.

Platzman, G.W., 1963: The dynamical prediction of wind tides on Lake Erie. Meteorol. Monographs, 4, No. 26, 44 pp.

Rotta, J. C., 1962: Turbulent boundary layers in incompressible flow. Progresses in Aerospace Sci., 2, 1-219.

Schwab, D.S., 1981: Determination of wind stress from water level fluctuations. Ph.D. thesis, U. of Michigan, 108 pp.

Simons, T.J., 1974: Verification of numerical models of Lake Ontario. I. Circulation in spring and early summer. J. Phys. Ocean., 4, 507-523.

Simons, T.J., 1975: Verification of numerical models of Lake Ontario. II. Stratified circulations and temperature changes. J. Phys. Ocean., 5, 98–110.

Smith, S.D., 1980: Wind stress and heat flux over the ocean in gale force winds. J. Phys. Ocean. 10, 709–726.

Smith, S.D., and E.G. Banke, 1975: Variation of the sea surface drag coefficient with wind speed. Quart. J. Roy. Meteor. Soc., 101, 665-673.

Timmerman, H., 1977: Meteorological effects on tidal heights in the North Sea. Mededelingen en Verhandelingen, Koninklijk Nederlands Meteor. Inst., 99, 105 pp.

Volkov, Yu A., 1970: Turbulent flux of momentum and heat in the atmospheric surface layer over a disturbed sea surface. Izv. Atmos. Oceanic. Phys., 6, 770–774.

Wieringa, J., 1980: A revaluation of the Kansas mast influence on measurements of stress and cup anemometer overspeeding. Bound.-Layer Meteor., 18, 411-430.